18th International Conference on the Application of Computer
Science and Mathematics in Architecture and Civil Engineering
K. Gürlebeck and C. Könke (eds.)
Weimar, Germany, 07–09 July 2009

CHARACTERIZATION OF TIME-DEPENDENT DEFORMATIONS OF POLYMER MODIFIED CEMENT CONCRETE (PCC)

H. Keitel*, A. Dimmig-Osburg and V. Zabel

**Research Training Group 1462*
Bauhaus-Universität Weimar
Berkaerstr. 9
99423 Weimar
Germany
E-mail: holger.keitel@uni-weimar.de

Keywords: PCC, Polymer Modified Cement Concrete, Creep

Abstract. *Tests on Polymer Modified Cement Concrete (PCC) have shown significant large creep deformation. The reason for that as well as additional material phenomena are explained in the following paper. Existing creep models developed for standard concrete are studied to determine the time-dependent deformations of PCC. These models are: model B3 by Bažant and Bajewa, the models according to Model Code 90 and ACI 209 as well as model GL2000 by Gardner and Lockman. The calculated creep strains are compared to existing experimental data of PCC and the differences are pointed out. Furthermore, an optimization of the model parameters is performed to fit the models to the experimental data to achieve a better model prognosis.*

1 INTRODUCTION

The characterization of time-dependent deformations of concrete structures has been subject of extensive research for many decades. So far various constitutive relations for the prediction of these deformations have been developed. The field of application is in most cases limited to standard concrete. Whether these models can be applied to special concrete, e.g. PCC, with its significant large creep deformations, will be investigated. In this paper the peculiarity of the material of PCC as well as the creep phenomenon are explained. Existing creep models using the compliance function are shown and their use for PCC instead of standard concrete is evaluated. Finally a parameter optimization is performed to verify if a modification of the existing constitutive equation results in a better agreement with the deformational behavior of PCC.

2 MATERIAL PHENOMENA OF PCC

Polymer Modified Cement Concrete is, especially because of its good adhesive tensile strength as well as of its high resistance to chemical loading, an important material for the restoration of concrete structures and even more as protection for concrete structures underneath [1]. It is also used for new buildings, e.g. industrial floors. It shows partially differing properties to usual Cement Concrete (CC) which will be explained in the next paragraphs.

The difference between PCC and CC in the concrete composition is that polymers are added to the fresh concrete. The addition of polymers to the concrete mix can be from 5% up to 15% of the cement content. The nature and the consistency of the polymer can vary. Usually, styrene-butadien and styreneacrylacidester are used as dispersion or redispersible powder. The nature and the consistency as well as the minimum filmfommation temperature (MFT) of the polymers have a large influence on the properties of the green and hardened concrete. For example the polymer modification leads to a softer consistency of the ready-mixed concrete [2], resulting in a better workability.

The effect of the modification also concerns the hydration of the cement. The polymers form a film network around the cement particles and decrease the water diffusion to the non-hydrated cement particles [1]. Consequently, the hydration processes decelerate significantly and the post-hardening is more pronounced. The polymers and the cement together form the binder matrix, the polymer phases interpenetrate the cement phases [3]. Furthermore, the void volume of the hardened concrete increases.

The properties of the hardened concrete are influenced by the afore mentioned phenomena. The Young's modulus and the compression strength decrease, the tensile and the flexural tensile strength increase up to a factor of two. The material shows a more ductile fracture behavior. The decelerated hydration and the increased void volume together with viscous properties of the polymer itself lead to significant viscous properties of the material. Which, in turn results in large time-dependent creep deformations.

Figure 1 shows the comparison of the longitudinal and transversal strains for a compression test of Standard Concrete (0-Probe) and Modified Concretes (PCC1, PCC2 and PCC4) at a

stress-level of 90% (CC) and 80% (PCC) of the short-time strength. It can be observed that the stiffness of the PCC decreases and the ductility increases. Another difference is the high creep deformation of the modified materials. Even for short load durations of 180 seconds the creep deformation is significant.

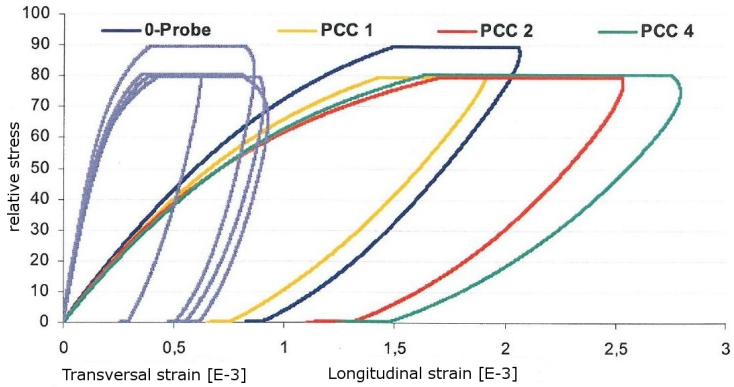

Figure 1: Comparison of compression tests of CC and different PCC for a load duration of 180s [4]

3 CREEP PHENOMENON AND MODELS

Creep is the time-dependent increase of strain due to a sustained loading. The creep rate is high at the beginning of loading. It decreases over time and the creep deformations seem to approach a final value for a loading below the creep resistance. If creep actually stagnates when time goes to infinity is still discussed nowadays. For a stress level above the creep resistance the creep rate does not decrease as $t \rightarrow \infty$. For that reason creep is divided into 3 phases: primary, secondary and tertiary creep (see Figure 2). For primary creep the deformations are linear to the applied stresses and the creep rate approaches approximately zero for $t \rightarrow \infty$. This phase is present up to a stress level of approximately 30%-40% of the short-term strength, which is equivalent to service loads. Secondary creep means that the deformations increase permantly over the time which results in tertiary creep, which is an increase in the creep rate and leads to failure of the concrete.

Some of the physical reasons of creep are the ongoing hydration of the cement particles and diffusing pore water. Depending on the boundary conditions creep can be divided into two parts: basic and drying creep. Basic creep occurs for equal humidity in the environment and the concrete. Drying creep (also called stress induced shrinkage or “Pickett effect”) is an additional creep deformation due to the drying of the concrete [6]. The emerging deformations are reversible visco-elastic and irreversible visco-plastic (flow).

The creep as well as the creep rate depend on many different parameters. The age τ of the concrete at loading is the main factor. As the concrete reaches maturity and the hydration processes are more progressed, the tendency to creep is reduced. The age t_d of the concrete at the beginning of drying has an influence on the drying creep as well as on the hydration processes. The concrete composition also affects the time-dependent deformations. This is characterized

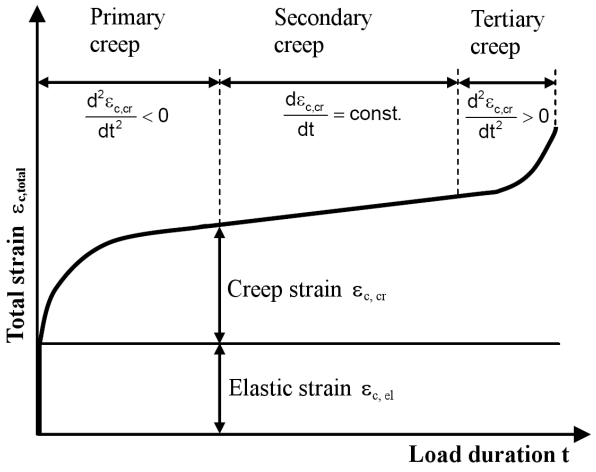

Figure 2: General form of strain-time diagram of the different creep phases [5]

by the strength, cement content, water-cement-ratio as well as the size and stiffness of the aggregates. More factors are the size and the shape of the concrete structure as well as the humidity.

The development of creep models has been part of extensive research for many decades. Various approaches that describe creep deformation have been developed and can be found in [7, 8, 9, 10, 11, 12, 13, 14]. These relations describe the increased strain over time by the creep coefficient $\phi_{cr}(t)$, which is the increase factor for the instantaneous elastic strains.

$$\epsilon_{cr}(t) = \phi_{cr}(t)\,\epsilon_{el} \tag{1}$$

The path of these functions varies from exponential, logarithmic, power and hyperbolic form as well as a combination of these types. These functions can be divided into two groups: using a summation-approach and a product-approach. The summation-approach adds several creep terms to one function (e.g. visco-elastic and visco-plastic deformations). The product-approach has a fixed creep value which is multiplied by a time function. A continuation of the approach of the creep coefficient is the definition of a compliance function $J(t)$ which considers the elastic and viscous deformations.

$$J(t) = \frac{1 + \phi_{cr}(t)}{E} \tag{2}$$

The compliance functions are the most common and practicable method to consider creep deformations in numerical calculations. These will be explained in detail in the next subsections. They are valid for constant loading and variable loading if linear creep can be assumed. Stress states that cannot be described are complete unloading and cyclic loading. To give information regarding the creep resistance as well as the stiffness degradation is not possible. For an analysis of the afore mentioned problems rheological models need to be used. These models are not part of this paper but can be found in the literature, for example published in [15, 16].

3.1 Existing Compliance Functions

As explained in the previous paragraph many different compliance functions already exist. For this paper four different creep models: B3, Model Code 90, ACI209 and GL2000 were considered and are described in the next subsections. The respective shrinkage models were not

explained in this paper but can be found in the literature [14, 17, 18, 19].

The model B3 is the most sophisticated model which combines several physical phenomena. The disadvantage is the need of many input parameters. The models according to Model Code 90 and ACI 209 use a product-approach with different time functions for each of the models. Depending on the input parameters the path and the final creep value can be shifted. GL2000 is the model that requires the least number of input parameters but giving nearly the same accuracy in creep prediction for standard concrete as the other models. Therefore, it is especially important for practical use in engineering practice.

3.1.1 Model B3 by Baẑant and Bajewa

The Model B3 by Baẑant and Bajewa [14, 20, 21] follows the summation-approach and divides the creep explicitly into visco-elastic and visco-plastic (flow) parts. Each of the physical mechanism – aging visco-elastic, non-aging visco-elastic, flow and drying creep – has its own time function. These are hyperbolic functions, logarithmic and logarithmic-power functions. The compliance is divided into basic creep compliance

$$C_0\left(t,\tau\right) = q_2 Q\left(t,\tau\right) + q_3 ln\left[1+\left(t-\tau\right)^n\right] + q_4 ln\left(\frac{t}{\tau}\right) \tag{3}$$

and drying creep compliance

$$C_d\left(t,\tau,t_d\right) = q_5\sqrt{e^{-8H(t,t_d)} - e^{-8H(\tau,t_d)}}. \tag{4}$$

$Q\left(t,\tau\right)$ is the time-function for the aging visco-elastic compliance. The function $H\left(\tau,t_d\right)$ is the spatial average of pore relative humidity within the cross section. The specific formulas can be found in [14]. The parameter n is $n = 0.1$.

The compliance becomes

$$J\left(t,\tau\right) = q_1 + C_0\left(t,\tau\right) + C_d\left(t,\tau,t_d\right). \tag{5}$$

The factors q_1 to q_5 are material parameters depending on water-cement-ratio w/c, aggregate-cement-ratio a/c, 28-day compression strength $f_{c,28}$, cement content c and the ultimate shrinkage strain $\epsilon_{sh\infty}$ and can be determined for standard concrete according to Equation 6.

$$\begin{aligned}
q_1 &= \frac{0.6}{E_{28}} = \frac{0.6}{1497\sqrt{f_{c,28}}} \\
q_2 &= 2.33\cdot 10^{-4}\, c^{0.5}\, f_{c,28}^{-0.9} \\
q_3 &= 0.29\left(\frac{w}{c}\right)^4 q_2 \\
q_4 &= 2.03\cdot 10^{-4}\,\left(\frac{a}{c}\right)^{-0.7} \\
q_5 &= \frac{1.90\cdot 10^{-4}}{f_{c,28}\,\epsilon_{sh\infty}^{0.6}}
\end{aligned} \tag{6}$$

Each of the factors has a phenomenological meaning: q_1 is the instantaneous compliance, q_2 is the aging visco-elastic compliance, q_3 is the non-aging visco-elastic compliance, q_4 is the flow

compliance and q_5 is the drying creep compliance. The influence of these parameters on the path of the compliance function is demonstrated in Figure 3 for the value of $q = 10^{-3}$ for each parameter.

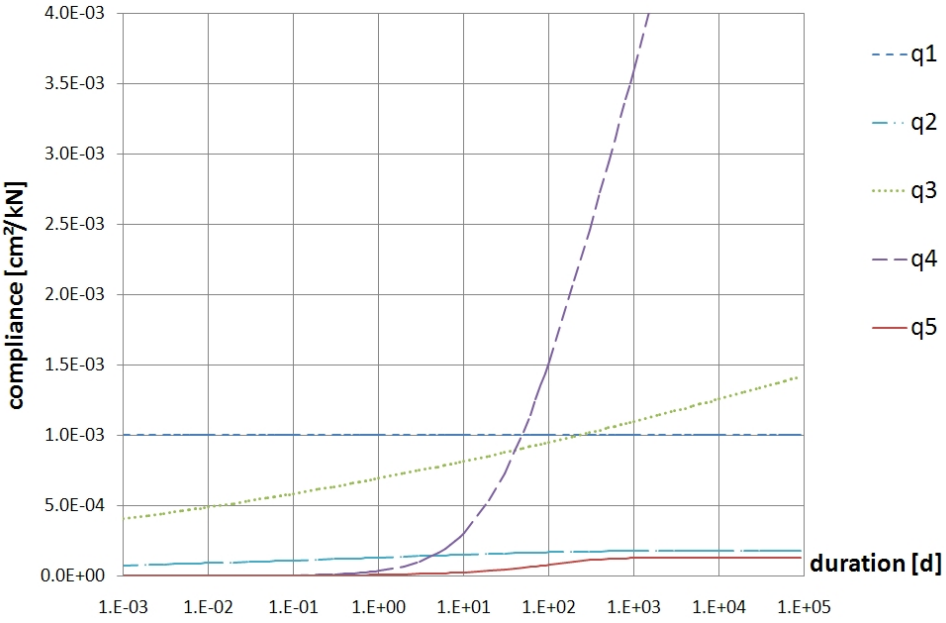

Figure 3: Path of the compliance for $q_1 ... q_5 = 10^{-3}$

The over-proportionality of the creep for stress rates of $0.4 f_c \leq \sigma \leq 0.6 f_c$ is considered with the factor

$$F(\sigma, f_c) = \frac{1 + 3\left(\frac{\sigma}{f_c}\right)^5}{1 - \left(\frac{\sigma}{f_c}\right)^{10}}, \tag{7}$$

which is multiplied with the creep compliances C_0 and C_d.

3.1.2 Model according to CEB Model Code 90

The model of the Model Code 90 [17] considers creep as an aging linear visco-elastic material. The creep formula follows the product formulation of the creep strains, multiplying a notional creep coefficient by a time function. With that the model assumes a final creep value. There is no distinction between basic and drying creep made. The creep coefficient is referring to the Young's modulus at the age of 28 days and has a hyperbolic shape.

$$\phi_{cr,28}(t, \tau_{eff}) = \phi_\infty \beta_c (t - \tau_{eff}) \tag{8}$$

with the final creep value

$$\phi_\infty = \phi_{RH} \beta(f_{cm}) \beta(\tau_{eff}) \tag{9}$$

and the path function

$$\beta_c\left(t-\tau\right)=\left[\frac{t-\tau}{\beta_{RH}+t-\tau}\right]^{0.3}. \tag{10}$$

Here $\beta\left(f_{cm}\right)$ is a factor considering the influence of the concrete strength; the factor $\beta\left(\tau_{eff}\right)$ takes into account the age of the concrete at the beginning of loading; β_{RH} considers the effect of humidity on the path of creep strain and ϕ_{RH} is a basic creep factor also depending on the humidity. The model has the advantage of taking into account the effective-age of the concrete at the beginning of loading. This is, especially for the PCC with a decreased rate of hydration, an important property of the model. The effective age τ_{eff} of the concrete at the beginning of loading is formulated depending on the temperature, which is not considered here, and the type of cement used

$$\tau_{eff}=\tau\left[\frac{9}{2+\tau^{1.2}}+1\right]^{\alpha} \tag{11}$$

with the power of α depending on the type of cement. The compliance function becomes

$$J\left(t,\tau\right)=\frac{1}{E_\tau}+\frac{\phi_{28}}{E_{28}}. \tag{12}$$

The non-linearity of the creep for high stress rates can be considered for the range of $0.4f_c \leq \sigma \leq 0.6f_c$ by using the over-proportionality factor

$$F\left(\sigma,f_c\right)=e^{1.5\left(\frac{\sigma}{f_c}-0.4\right)}. \tag{13}$$

3.1.3 Model according to ACI 209

The creep formula of the American Concrete Institute [18] follows the product formulation of the creep strains, considering a final creep value and multiplying this with a time function. No distinction between basic and drying creep is made. The creep coefficient refers to the Young's modulus of the concrete at the beginning of loading E_τ. The shape of the function is hyperbolic-power and mainly determined by the exponent ψ.

$$\beta\left(t,\tau\right)=\frac{\left(t-\tau\right)^{\psi}}{d+\left(t-\tau\right)^{\psi}} \tag{14}$$

For standard concrete are $\psi=0.6$ and $d=10\ days$. For $\psi=1$ the path of the function is nearly similar to Ross [9] and Lorman [10]. The final creep value ϕ_∞ can be calculated by multiplying a basic value by correction factors

$$\phi_\infty=2.35\,\gamma_\tau\,\gamma_{RH}\,\gamma_h\,\gamma_T\,\gamma_{slump}\,\gamma_{void}. \tag{15}$$

These correction factors consider the age of concrete at loading, γ_τ, the humidity, γ_{RH}, the average member size, γ_h, the temperature, γ_T, the slump of the fresh concrete, γ_{slump} and the void volume, γ_{void}.

The compliance function results to

$$J(t,\tau) = \frac{1}{E_\tau} + \frac{\frac{(t-\tau)^\psi}{d+(t-\tau)^\psi}\phi_\infty}{E_\tau}. \tag{16}$$

The non-linearity of the creep for high stress rates is not taken into account.

3.1.4 Model GL2000 by Gardner and Lockman

The model by Gardner and Lockman [19] is a creep prediction model which is well applicable in engineering practice. The advantage is the availability of all input parameters. Only the 28-day compression strength $f_{c,28}$, the concrete strength at loading $f_{c,\tau}$, the humidity RH and element size expressed by the volume-surface ratio $\frac{V}{S}$ are necessary. Instead of $f_{c,28}$ and $f_{c,\tau}$, E_{28} and E_τ can be used. This model has no final creep value which distinguishes it from MC90 and ACI209. It combines hyperbolic and power functions and takes into account the drying before loading. The creep coefficient is referring to Young's modulus at the age of 28 days E_{28}.

$$\begin{aligned}\phi_{28} = \Phi(t_c) &\left[2\left(\frac{(t-\tau)^{0.3}}{(t-\tau)^{0.3}+14}\right) + \left(\frac{7}{\tau}\right)^{0.5}\left(\frac{t-\tau}{t-\tau+7}\right)^{0.5}\right] \\ +\Phi(t_c) &\left[2.5\left(1-1.086RH^2\right)\left(\frac{t-\tau}{t-\tau+0.15\left(\frac{V}{S}\right)^2}\right)^{0.5}\right]\end{aligned} \tag{17}$$

The parameter $\Phi(t_c)$ takes account of the drying before loading ($t_d \leq \tau$) and can be determined by

$$\Phi(t_c) = \left[1 - \left(\frac{\tau - t_d}{\tau - t_d + 0.15\left(\frac{V}{S}\right)^2}\right)^{0.5}\right]^{0.5}. \tag{18}$$

The compliance function is similar to Equation(12). The non-linearity of the creep for high stress rates is not considered.

3.2 Assessment of the Influence of Parameters

In the following the influence of certain physical concrete parameters on the compliance function is shown by using model B3. The different parameters affect the time-dependent aging and flow effects. Hence the influence of these parameters on the compliance is time-dependent, too. For the following graphs all input parameters except the observed one are kept constant and are shown in Table 1. In these diagrams it is not considered that the parameters correlate with other parameters, for example the influence of the water-cement-ratio on the concrete strength.

Figure 4 shows the influence of the 28-day concrete strength. An increase in strength, which is equivalent to an increase in the Young's modulus, decreases the instantaneous strains. Apart from the instantaneous strains the creep strains and the creep coefficient are also reduced. Figure

$f_{c,28}$ $\frac{kN}{cm^2}$	τ d	t_d d	RH %	c $\frac{kg}{cm^3}$	$\frac{w}{c}$ $-$	$\frac{a}{c}$ $-$
4.0	28	7	65	350	0.5	5

Table 1: Parameters for comparison of compliance function

5 reveals that a higher cement content results in higher creep deformations assuming a constant concrete strength. The cause for this is a larger cement-paste fraction in the concrete and this is the phase where creep occurs. The higher the water-cement ratio (Figure 6)is, the greater the creep will be. This results from the increased drying creep as well as the more viscous properties of the cement paste. A larger aggregate-cement ratio decreases the time-dependent deformation. This is because the aggregates do not creep unlike the cement paste (Figure 7). The last parameter observed is the humidity (Figure 8). The lower this value is the more water from the concrete is emitted into the environment. This results in larger drying creep and shrinkage.

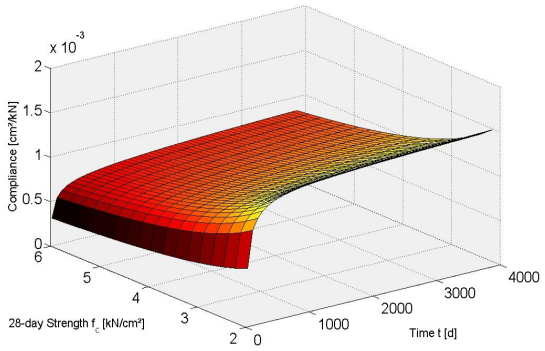

Figure 4: Compliance J depending on $f_{c,28}$ and t

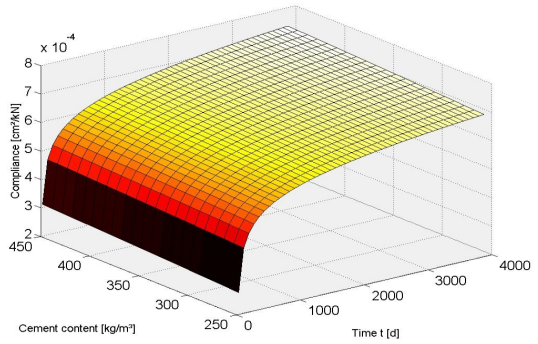

Figure 5: Compliance J depending on c and t

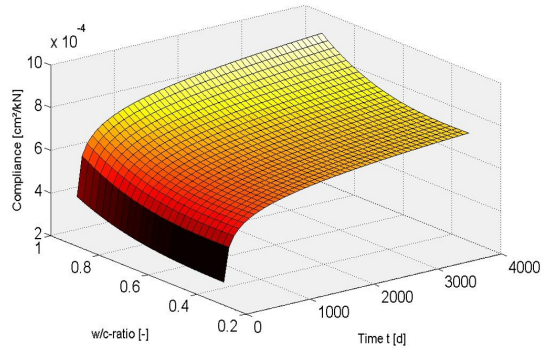

Figure 6: Compliance J depending on $\frac{w}{c}$ and t

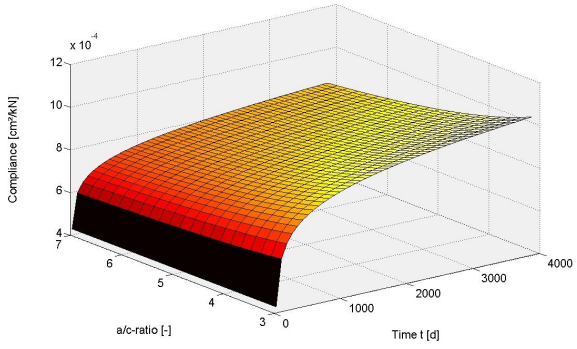

Figure 7: Compliance J depending on $\frac{a}{c}$ and t

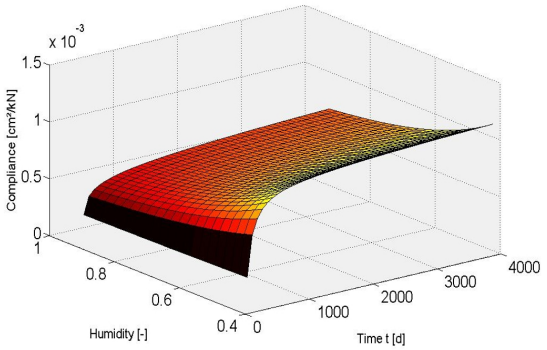

Figure 8: Compliance J depending on RH and t

4 APPLICATION OF THE MODELS TO PCC

In this section the previously mentioned creep models were used to determine the time-dependent behavior of PCC. Because of the differences in CC and PCC a significant deviation of the model prognosis to the experimental data is expected. The deviation is expressed in terms of the variation coefficient $\overline{\omega}$ explained in section 4.2.

4.1 Long-Term Tests of PCC

In this paper two long-term compression tests of PCC were considered for the creep calculations. These tests are uni-axial compression tests of concrete cylinders with a diameter $d = 10\ cm$ and a height of $h = 30\ cm$. The experiments were conducted by Flohr [4, 22]. The polymer used for both tests is a styreneacrylacidester as a redispersible powder (called PCC2). The cement is CEM I. The boundary conditions of the experiments and the concrete compositions are shown in Table 2. The sign convention for compression stress is positive.

	dura-tion d	$f_{c,28}$ $\frac{kN}{cm^2}$	$f_{c,\tau}$ $\frac{kN}{cm^2}$	σ $\frac{kN}{cm^2}$	τ d	t_d d	RH %	c $\frac{kg}{cm^3}$	$\frac{w}{c}$ –	$\frac{p}{c}$ –	$\frac{a}{c}$ –	a %	s cm
Test 1	33	2.62	4.13	1.64	75	7	65	350	0.50	0.15	4.85	5.9	60
Test 2	154	2.62	≈4.2	2.48	265	7	65	350	0.50	0.15	4.85	5.9	60

Table 2: Existing long-term compression tests of PCC2 [4, 22]

Due to the humidity of less then 100% the concrete specimens exhibited basic creep, drying creep and shrinkage. Basic and drying creep are determined with the mentioned models. For the calculation of shrinkage the corresponding shrinkage models for standard concrete were used. The shrinkage strain of these experimental tests are very small compared to the creep strains. Consequently, the influence of shrinkage on the deformation is minor. The temperature during the element tests was 20°C. The reference temperatures for the creep models are in the range of 20°C-23°C. Accordingly the influence of the temperature can be neglected.

4.2 Coefficient of Variation $\overline{\omega}$

The difference between the model prognosis and the experimental results are compared using the variation coefficient $\overline{\omega}$ according to [20]. It takes account of different numbers of experimental data points for different logarithmic time decades using a weighting function w_i. With that function each time decade has the same influence on the variation coefficient regardless of the number data of points in that decade.

$$w_i = \frac{n}{n_d n_i}, \qquad \sum_{i=1}^{n} w_i = n \tag{19}$$

Here n is the number of total data points; n_d is the number of decades on the logarithmic time scale spanned by the measured data and n_i is the number of data points in the decade the data point i belongs to. The deviation of the strains of the model to the experiment for the data point i is expressed by

$$\Delta_i = \epsilon_{exp}(t_i) - \epsilon_{cal}(t_i) = \epsilon_{exp}(t_i) - \epsilon_{cr,cal}(t_i) - \epsilon_{sh,cal}(t_i) + \epsilon_{sh,cal}(\tau). \tag{20}$$

Furthermore, the measured strain values $\epsilon_{exp,i}$ are considered to ensure the same impact for small absolute, but large relative strain differences, e.g. for short time creep. The variation coefficient becomes

$$\overline{\omega} = \frac{s}{\overline{\epsilon}_{exp}} = \frac{1}{\overline{\epsilon}_{exp}} \left[\frac{1}{n-1} \sum_{i=1}^{n} \left(w_i \Delta_i \right)^2 \right]^{\frac{1}{2}}, \tag{21}$$

with

$$\overline{\epsilon}_{exp} = \frac{1}{n} \sum_{i=1}^{n} w_i \epsilon_{exp,i}. \tag{22}$$

The coefficient $\overline{\omega}$ is a figure of merit for the deviation of the strains of the test data to the calculation.

4.3 Results of Calculations

For the calculations of the creep deformations the parameters were determined for standard concrete. The decisive parameters, which are used for the optimization later on, are shown in Tables 4 and 5. Figures 9 and 10 demonstrate the resulting time-dependent strain in conjunction with experimental data.

For test 1 the calculated creep deformations are much smaller than the measured for load durations exceeding one day. Even for several hours of loading the strain is underestimates in the B3, GL2000 and ACI models. The MC90 model overestimates this short-term creep. Looking at the path of strain and not at the values themselves, the deviations of the models B3, MC90 and GL2000 to the experiment are obvious. The creep rates for these models decrease much faster than in the experiment or even in model ACI. This results in a graph with minor slope. The resulting coefficients of variation are shown in Table 3.

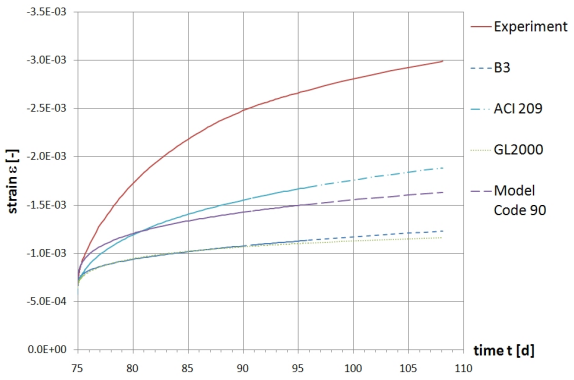

Figure 9: Comparison of calculated and measured strains (Test 1)

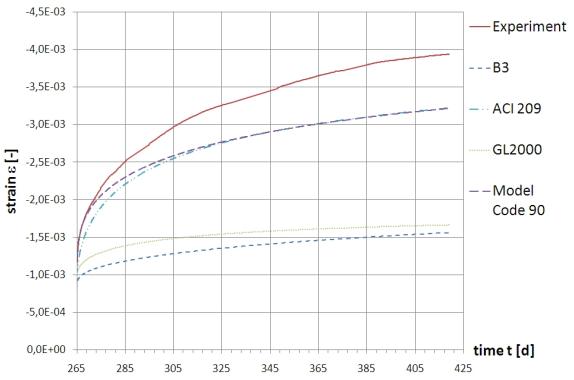

Figure 10: Comparison of calculated and measured strains (Test 2)

The comparison for test 2 shows that the models MC90 and ACI can reproduce the creep deformations better then B3 and GL2000, which completely underestimate the strain. In B3 and GL2000 models almost no creep strain occurs. While the creep strain predicted by MC90 and ACI models are larger, they cannot reproduce the creep curves in an reasonable way. The creep rate, especially at the ending of the test, is higher for the PCC as predicted by the models and the shape of the function is not reproduced very well.

	Model B3	ACI 209	GL2000	Model Code 90
Test 1	0.6491	**0.5037**	0.7077	0.6116
Test 2	0.5207	**0.1751**	0.4603	0.1872

Table 3: Variation coefficients $\overline{\omega}$ for different models

Comparing test 1 and test 2 it is evident that test 2 can be reproduced better by some of the models. The cause is the high age of concrete at loading. The post hardening of the PCC is more progressed and the degree of hydration is higher, so that the viscous properties are reduced.

5 OPTIMIZATION OF MODEL PARAMETERS

As mentioned in the previous section using models developed for CC results in large discrepancies between the calculated and measured deformations of PCC. Theses discrepancies are due to the different shapes of the time function for CC and PCC and a different scale of the creep values. In this section the parameters of the models are optimized to minimize the objective function, which is the coefficient of variation $\overline{\omega}$. This will minimize the deviations of the calculated and measured strains.

The parameters of the optimization depend on the various creep models. For the B3 model, Baẑant and Bajewa [14] suggest to optimize the material parameters $q_1 ... q_5$, which consider the concrete composition. Due to the polymer modification the concrete composition of PCC can-

not be compared to CC. Consequently $q_1 ... q_5$ need to be optimized for PCC. The shape of the time functions (Figure 3) is not modified. The optimization parameters of the ACI 209 model are according to [18] the exponent ψ and the addend of the denominator d as well as the final creep value ϕ_∞. The MC90 model does not include any parameters to influence the shape of the time-function. The only parameter to calibrate in this model is the final creep value ϕ_∞. An optimization of the single parameters ϕ_{RH}, $\beta\left(f_{cm}\right)$ and $\beta\left(\tau_{eff}\right)$, which define ϕ_∞ (Equation (9)), is not possible. The cause is that only the product of all parameters is decisive and thus no reasonable results of a single parameter would be obtained. Consequently, the value of single parameters cannot be determined by that optimization. The GL2000 model does not give any opportunity to optimize the creep curve. The causes are the fixed input parameters like the geometric properties, the humidity and the concrete strength.

5.1 Results of Optimization

The results of the parameter optimization using quasi-Newton algorithms are shown in Tables 4 and 5 as well as in Figures 11 and 12. The graphs show a good agreement of the calculated and measured data for the B3 and ACI models. The coefficient of variation (Table 6) becomes very small. The MC90 model overestimates the creep for short loading periods and underestimates the deformations for long loading periods. The shape of the curve cannot be optimized for that model. Consequently, it is not able to demonstrate the specific time dependent behavior of polymer modified cement concrete.

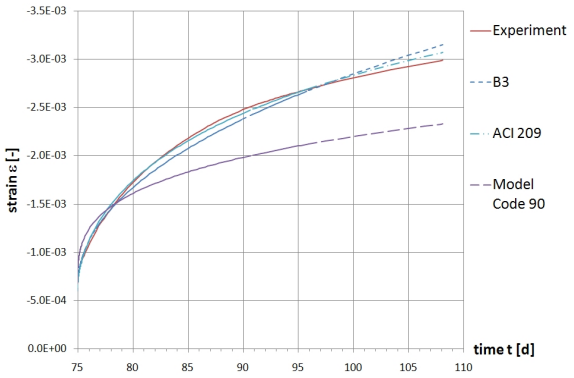

Figure 11: Comparison of strains after optimization (Test 1)

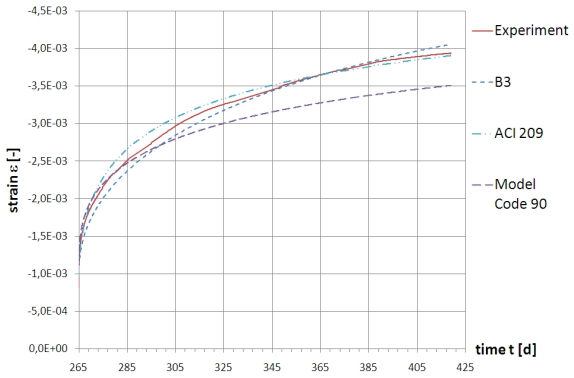

Figure 12: Comparison of strains after optimization (Test 2)

Comparing only the curves in Figures 11 and 12 as well as the variation coefficient the result of that optimization would be that the existing compliance functions in B3 and ACI could be used for the calculation of PCC, since their curves fit reasonably well and the coefficient of variation is low. But a detailed analyzes of the results reveals some discrepancies which are explained in the following.

One disadvantage of the optimization of time-dependent strains is that the creep rate is not explicitly part of the optimization. This becomes obvious when comparing the curves of test 1 with the short load duration of 33 days. The creep rate, equivalent to the gradient of the curve,

Model B3			ACI 209			Model Code 90		
Param.	Model	Optim.	Param.	Model	Optim.	Param.	Model	Optim.
q_1	2.48E-4	3.17E-4	Ψ	0.60	1.00	ϕ_∞	2.56	3.70
q_2	1.84E-3	1.21E-3	d	10.00	30.01			
q_3	3.34E-5	1.00E-9	ϕ_∞	3.99	8.11			
q_4	6.72E-5	1.00E-9						
q_5	5.23E-3	5.89E-2						

Table 4: Parameters according to model and after optimization (test 1)

Model B3			ACI 209			Model Code 90		
Param.	Model	Optim.	Param.	Model	Optim.	Param.	Model	Optim.
q_1	2.48E-4	2.80E-4	Ψ	0.60	0.55	ϕ_∞	2.06	4.54
q_2	1.84E-3	2.95E-3	d	10.00	8.37			
q_3	3.34E-5	1.00E-9	ϕ_∞	3.44	4.61			
q_4	6.72E-5	1.00E-9						
q_5	5.23E-3	3.67E-2						

Table 5: Parameters acc. to model and after optimization (test 2)

at the time of 108 days (33 days of load duration) is much higher for the B3 and ACI models than for the experiment, even if the curves fit reasonable. Consequently, the models overestimate creep for loading periods larger than the time of the experiment. Therefore, these model parameters are only valid for load durations similar to the experiment.

Another shortcoming becomes visible comparing the parameters of tests 1 and 2 at Tables 4 and 5. For the B3 model the parameters $q_1 ... q_5$ depend on the material composition, which is equal both for tests 1 and 2. Thus the parameters should be similar. Comparing especially the values of q_2 and q_5 differences occur. The reason for that is the specific creep behavior of PCC. The creep of PCC is, especially for short load durations of a few days up to several weeks, significant high. The parameters for the 33-day testing are calibrated for these large creep values. The long-term creep of PCC is not as significant large as the short-term creep. Therefore, the parameters for prediction of the long-term deformations are smaller after optimization. This problem is also shown by the model according to ACI. The predicted final creep value ϕ_∞ for the short load duration of test 1 is much greater than that of test 2. The reason is again due to the high short-term creep of PCC which results in an overestimation of the long-term creep.

Another problem is the poor determinability of the parameters q_3 and q_4 for the B3 model. This fact can be due to the relative low sensitivity of these parameters for the time decades smaller then 10 days (see Figure 3), especially for q_3. The analysis of long-term creep tests with load durations longer than 1000 days could prove that statement. An additional reason might be that the time functions which belongs to these parameters are not valid for PCC.

	Model B3	ACI 209	Model Code 90
Test 1	**0.0433**	0.2768	0.5355
Test 2	0.0857	**0.07670**	0.1747

Table 6: Variation coefficients $\overline{\omega}$ after optimization

6 CONCLUSION

Creep models for Standard Concrete were studied to determine their use for Polymer Modified Cement Concrete. The B3 model by Bažant and Bajewa, the models according to Model Code 90 as well as ACI 209 and GL2000 model by Gardner and Lockman were examined. The model prediction is compared with existing experimental data.

There is a large deviation of the measured creep strain values from the calculated values when using CC input parameters for PCC. The most notable underestimation is the creep within the first 3-4 weeks. For long-term creep certain models, MC 90 and ACI 209, predict larger creep values then others, like B3 and GL2000 model. However the measured strain of PCC greatly exceed the estimates of all models notably.

To improve the prediction of creep of these models the input parameters of the models B3, MC 90 and ACI 209 were optimized to minimize the coefficient of variation. With this optimization the deviations of measured and calculated strain were reduced. The curve of the experimentally determined data can be described with B3 and ACI 209 model. Discrepancies occur when comparing the parameter's results of both analyzed creep tests. The parameters are dependent on the duration of the creep experiment. To avoid this, creep experiments emphasizing extended loading periods should be considered. Furthermore, the weighting function proposed by Bažant and Bajewa could be modified to emphasize larger load durations in the optimization process.

For a generalized statement on the use of the existing compliance function for PCC more experiments, respectively the back analysis of these experiments, are necessary.

In order to assess the quality of creep prediction models, the sensitivity towards the input parameters and the robustness of the models will be analyzed. Furthermore the variation of the calculated creep strain due to uncertainties of the input parameters is investigated. This will answer the question whether sophisticated models, requiring many input parameters including uncertainties, predicted lower variation of the strains than simple models considering only a minimum of input parameters. With these and further information general statements towards the quality of creep models will be derived.

REFERENCES

[1] Y. Ohama. *Handbook of Polymer-Modified Concrete and Mortars*. Noyes Publications, 1995.

[2] A. Chandra and Y. Ohama. *Polymers in Concrete*. CRC Press, Inc., 1994.

[3] A. Dimmig. *Einflüsse von Polymeren auf die Mikrostruktur und die Dauerhaftigkeit kunststoffmodifizierter Mörtel (PCC)*. Dissertation, Bauhaus-Universität Weimar, 2002.

[4] A. Flohr. Stoffliche Aspekte des Einflusses einer Polymermodifikation auf die statischen und dynamischen Eigenschaften von Konstruktionsbeton. Diploma's thesis, Bauhaus-Universität Weimar, 2005.

[5] J.-H. Shen. Lineare und nichtlineare Theorie des Kriechens und der Relaxation von Beton unter Druckbeanspruchung. In *Deutscher Ausschuss für Stahlbeton - Heft 432*. Beuth Verlag GmbH, 1992.

[6] Z.P. Bažant, A.B. Hauggaard, S. Baweja, and F.-J. Ulm. Mircoprestress-Solidification Theory for Concrete Creep. I: Aging and Drying Effects. *Journal of Engineering Mechanics*, 123 (11):1188–1194, 1997.

[7] F. Dischinger. Untersuchungen über die Knicksicherheit, die elastische Verformung und das Kriechen des Betons bei Bogenbrücken. *Der Bauingenieur*, 18:487–520, 539–552, 595–621, 1937.

[8] R. Pfefferle. *Zur Theorie des Betonkriechens*. Dissertation, Universität Karlsruhe, 1971.

[9] A.D. Ross. Concrete Creep Data. *The Structural Engineer*, 15(8):314–326, 1937.

[10] W.R. Lorman. Theory of Concrete Creep. In *Proceedings ASTM 40*, 1940.

[11] L.G. Straub. Plastic Flow in Concrete Arches. In *Proceedings ASCE 95*, 1931.

[12] J.R. Shank. The Plastic Flow of Concrete. In *Ohio State University Eng. Exp. Sta. Bull. 91*, 1935.

[13] Z.P. Bažant and E. Osman. Double Power Law for Basic Creep of Concrete. *Materials and Structures*, 9(49):3–11, 1976.

[14] Z.P. Bažant and S. Bajewa. Creep and Shrinkage Prediction Model for Analysis and Design of Concrete Structures - Model B3. *Materials and Structures*, 28:357–365, 1995.

[15] T. Heidolf. *Zeit- und beanspruchungsabhängiges Tragverhalten von polymermodifiziertem Beton unter mehrfach wiederholter Beanspruchung*. Dissertation, Bauhaus-Universität Weimar, 2007.

[16] J. Bockhold. *Modellbildung und numerische Analyse nichtlinearer Kriechprozesse in Stahlbetonkonstruktionen unter Schädigungsaspekten*. PhD thesis, Ruhr-Universität Bochum, 2005.

[17] Comite Euro-International du Beton. CEB-FIP Model Code 1990. Technical report, Comite Euro-International du Beton, 1993.

[18] ACI209. Prediction of Creep, Shrinkage, and Temperature Effects in Concrete Structures. Technical report, American Concrete Institute, 1992.

[19] N.J. Gardner and M.J. Lockman. Design Provisions for Drying Shrinkage and Creep of Normal-Strength Concrete. *ACI Materials Journal*, 98:159–167, 2001.

[20] Z.P. Bažant and S. Bajewa. Justificaton and Refinements of Model B3 for Concrete Creep and Shrinkage 1. Statistics and Sensitivity. *Materials and Structures*, 28:415–430, 1995.

[21] Z.P. Bažant and S. Bajewa. Justificaton and Refinements of Model B3 for Concrete Creep and Shrinkage 2. Updating and Theoretical Basis. *Materials and Structures*, 28:488–495, 1995.

[22] A. Flohr. Long-Term Creep Test of PCC. Experimental Test at the Junior Professorship "Polymer Binders and Building Materials in the Building Industry" at the Bauhaus-Universität Weimar - unpublished.